

# Discovery of an X-ray Emitting Nebula around the Recurrent Nova T Pyxidis

Ş. Balman

*Middle East Technical University, Physics Department, Inonu Bulvari, 356531, Ankara, Turkiye*

solen@astroa.physics.metu.edu.tr

## ABSTRACT

I resolved and detected an X-ray nebulosity around the recurrent nova T Pyx using a 98.8 ksec observation with the ACIS-S detector on-board the *Chandra* Observatory during the quiescent phase of the nova before its outburst in 2011. The nebula shows an elliptical shape with an inner semi-major axis  $\sim 0.45$  arc sec and an outer semi-major axis  $\sim 0.9$  arc sec which indicates a torus-like or a ring-like shell structure around the nova. There is also a (conical) elongation towards the southern direction of about 1.85 arc sec. This structure may be part of a bipolar outflow from the source/nova. The count rate of the nebulosity is  $0.0025 \pm 0.0010$  c s $^{-1}$  and that of the central binary is  $\sim 0.003$  c s $^{-1}$  over the 0.2-9.0 keV energy range. The best fitted spectrum of the X-ray nebula is a two-component plasma model (e.g., a double MEKAL) with  $\sim 0.6$  keV and  $\sim 2.2$  keV along with two different neutral hydrogen column densities of  $(0.2-0.9) \times 10^{22}$  cm $^{-2}$  and  $(3.0-26.0) \times 10^{22}$  cm $^{-2}$  for the two temperatures, respectively. I calculate an absorbed X-ray flux of  $(0.6-10.0) \times 10^{-14}$  erg cm $^{-2}$  s $^{-1}$  with a luminosity of  $(0.08-2.0) \times 10^{32}$  erg s $^{-1}$  (at 3.5 kpc) for the X-ray nebula. The estimated shocked mass is  $\leq 1.8 \times 10^{-5} M_{\odot}$ . The central source spectrum can be fitted by a single MEKAL model with a temperature  $9.2_{-5.4}^{\leq}$  keV yielding a luminosity of about  $5.2 \times 10^{31}$  erg s $^{-1}$ . The orbital period of the system is detected in the *Chandra* light curve.

*Subject headings:* X-rays: stars — radiation mechanisms: thermal — supernova remnants — shock waves — binaries: close — novae, cataclysmic variables — stars: Individual (T Pyxidis)

## 1. INTRODUCTION

Classical (CN) and recurrent (RN) nova outbursts occur as a result of thermonuclear runaways (i.e., explosive ignition of accreted material) on the surface of the white dwarf (WD)

primaries in cataclysmic variable (CV) systems ejecting material in a range  $10^{-7}$  to  $10^{-3} M_{\odot}$  with velocities from several hundred to several thousand kilometers per second (Shara 1989; Livio 1994; Starrfield 2001; Bode & Evans 2008). RN outbursts occur with intervals of several decades (Bode & Evans 2008). Nova outbursts show two main components of X-ray emission; a soft component dominating below 1 keV originating from the hot post-outburst WD and a hard component emitting above  $\sim 1$  keV as a result of accretion, wind-wind and/or blast wave interaction (Krautter 2008). The hard X-rays are mainly caused by the shocked plasma emission having plasma temperatures in a range 0.1-10 keV with luminosities  $\leq \text{afew} \times 10^{36}$  erg s $^{-1}$  *in the outburst stage* (Balman, Krautter, Ögelman 1998, Mukai & Ishida 2001, Orío et al. 2001; Bode et al. 2006; Sokoloski et al. 2006; Hernanz & Sala 2002,2007; Ness et al. 2009; Drake et al. 2009; Page et al. 2010; Vaytet et al. 2011; Orlando & Drake 2012; Nelson et al. 2012). There has only been one resolved and detected old CN remnant (GK Persei; Nova Per 1901) in the X-rays using  $\sim 100$  ksec *Chandra* observation (Balman 2005; Balman & Ögelman 1999). In addition, some extension in the radial profiles of the X-ray emission was recovered using the *Chandra* data of the recurrent nova RS Oph, one and a half years after the outburst possibly associated with the infrared and radio emitting regions (Luna et al. 2009). Recently, Balman (2010) detected extended X-ray emission in the radial profiles of the recurrent nova T Pyx using the *XMM-Newton* EPIC pn data.

T Pyx had five outbursts in 1890, 1902, 1920, 1944, and 1966 with an inter outburst time of  $19 \pm 5.3$  yrs (Webbink et al. 1987). A new quite delayed outburst occurred on April 14, 2011 (Waagan et al. 2011) and was observed over the entire electro-magnetic spectrum including the X-rays (Kuulkers et al. 2011a, 2011b). Ground-based optical imaging of the shell of T Pyx shows expansion velocities of about 350-500 km s $^{-1}$  (Shara et al. 1989; O’Brien & Cohen 1998). *Hubble Space Telescope* (HST; 1994-2007) observations of the shell show thousands of knots in H $\alpha$  and [NII] with expansion velocities of 500-715 km s $^{-1}$  that have not decelerated and the main emission is within a radius of 5'' (Shara et al. 1997; Schaefer, Pagnotta & Shara 2010). The joint UV, optical and the IR continuum spectrum of the binary system can be modeled using a blackbody of T  $\sim 34000$  K with  $\dot{M} \sim 10^{-8} M_{\odot} \text{ yr}^{-1}$ , dominated by the accretion disk (Gilmozzi & Selvelli 2007; Selvelli et al. 2008).

## 2. Observations and data reduction

T Pyx was observed using the *Chandra* (Weisskopf, O’dell, & van Speybroeck 1996) Advanced CCD Imaging Spectrometer (ACIS; Garmire et al. 2000) for a total of  $\sim 98.8$  ksec on three different pointings: 2011 January 31 (UT 16:22:36), 2011 February 2 (UT 03:05:41), and 2011 February 5 (UT 22:33:52) (PI=S. Balman). I used S3 (the back-illuminated CCD)

with the FAINT mode, and no gratings, yielding a moderate non-dispersive energy resolution. The ACIS has an unprecedented angular resolution of  $0''.49$  per pixel (half-power diameter). The ACIS PSF has a radius of  $0''.418$  (i.e., resolution) at 50% encircled energy which I exploit to recover the X-ray nebulosity around T Pyx.

The pipeline-processed data (aspect-corrected, bias-subtracted, graded and gain-calibrated event lists) are used for the analysis, and *acis-process-events* thread is used when necessary with the aid of CIAO 4.3 and a suitable CALDB 4.4.2 . For further analysis, HEASOFT version 6.9 is utilized. In order to double check, the archived data of T Pyx in February 2012 is also analyzed using CIAO 4.4 and CALDB 4.4.8.

### 3. Analysis and Results

#### 3.1. The X-ray Nebula around T Pyx

The *Chandra* observations of T Pyx were obtained in three sets (see section 2). The observations were merged with the standard procedures using a specific RA-DEC to match the three OBSIDs projecting the events to the nominal point of ACIS-S. Next, shifts were determined for the correction of the aspect solutions, updating WCS (World Coordinate System) and re-projecting the events matching them to the second observation (already projected to the nominal point of ACIS-S). At the end an aspect corrected and merged event file was generated. In order to create the PSF (Point Spread Function) MARX version 4.5.0 was used to run the CHART ray tracer using the necessary off axis angles, and the source spectrum and exposure time. Next, the PSF rays were projected onto the detector plane and finally an events file was generated for the source PSF. I have analyzed the T Pyx data generated in 2011 (processed with pixel adjustment set to randomize) and archived in 2012 (processed with pixel adjustment set to EDSE) and found similar results.

The standard *Chandra* resolution does not properly resolve the extended emission. The images calculated with 0.1 pixel resolution (sub-pixel resolution) reveal the structure better. The images created from the merged events file and the PSF events file with the above pixel resolution were smoothed by  $2 \times 2$  pixels using the task *csmooth* (using a Gaussian kernel) yielding a final image resolution of  $0''.15$ . Finally, the PSF image with the same spatial resolution was subtracted from the image of the merged events file while matching coordinates. The resulting subtracted images are displayed in Figure 1. The left hand panel shows the unsubtracted merged event file image, the middle panel shows the PSF-subtracted final image. In order to access the resulting nebular emission better, I also created an image from the brightest part of the spectrum between 1.0-2.0 keV with the same

sub-pixel resolution yielding a final image resolution of  $0''.15$ . The PSF-subtracted image in the 1.0-2.0 keV band is displayed on the right hand panel of Figure 1. The resulting images show extended emission with an elliptical shape. The inner semi-major axis is  $\sim 0''.45$  and the outer semi-major axis is  $\sim 0''.9$ . The inner semi-minor axis is  $\sim 0''.2$  and the outer semi-minor axis is  $\sim 0''.4$ . This indicates a torus-like or ring-like structure around the nova. There is also an elongation towards the south extending about  $1''.85$  from the point source. I note that this structure is not co-spatial with any HRMA artifacts. Moreover, I checked the consistency of the X-ray nebula in the individual observations by analyzing the three datasets and subtracting the PSF from each image. Though the S/N of the images are only 1/3 the total image, structures resembling Figure 1 were obtained.

I determined an approximate nebular and point source count rate by subtracting the PSF from the total image (merged) of the nebula within about a radius of  $5''.2$ . In the subtraction process, I used either  $1\times 1$  or  $2\times 2$  pixel smoothing for both the PSF and the total source images with the 0.1 pixel resolution, to account for the positional uncertainties of the photons (or anomalies in the PSF). I used a similar size photon extraction region obtained elsewhere in the images to account for the number of background photons. This yields a net count rate of  $0.0025\pm 0.0010$  c s $^{-1}$  (about 40% error) for the extended emission and  $\sim 0.003$  c s $^{-1}$  for the central source over the 0.2-9.0 keV energy range.

### 3.2. The *Chandra* Spectrum of the X-ray Nebula and the Central Source

In order to obtain a total spectrum from the three data sets of T Pyx, first, I derived the source+background spectra and the background spectra (using CIAO task *specextract*) for the individual observations using a photon extraction radius of  $5''.2$ . Next, I combined the spectra using the CIAO task *combine-spectra*. The resulting total spectrum is displayed in the top panel of Figure 2. Since the nebular emission is less than  $2''$  (total extend) around the point source a successful deconvolution of the spectrum of the nebular emission and the point source can not be made using the standard data extraction techniques using CIAO. Instead, I used the technique described below:

The combined spectrum of T Pyx were re-binned to have 16 energy channels across the 1024 channels of the *Chandra* ACIS-S. Next, I created images for each of the given 16 energy channel ranges using the merged events file and the PSF events file. Next, the PSF images created at the given energy channel ranges and smoothed by  $3\times 3$  pixels (using a Gaussian kernel) were removed from the images created at the same channel ranges (with the same smooting) using the merged events file. Resulting images were thresholded to have zero counts for the negative pixel values. Using these images, the number of counts

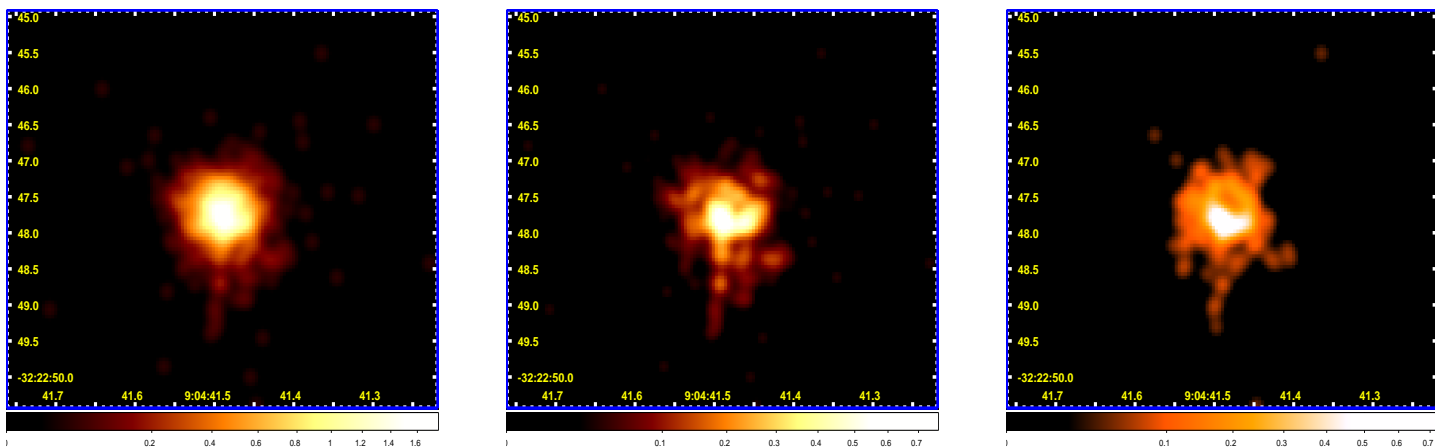


Fig. 1.— The X-ray images of T Pyx Nebula in the 0.2 to 7.0 keV range. The resolution is  $0.''15$  per pixel. North is up and West is to the right. The left hand panel is the 0.2-7.0 keV image without subtraction of the central source PSF. The middle panel is the PSF-subtracted image from the left hand panel. The image on the right hand panel is the PSF subtracted image in the 1.0-2.0 keV range. The axes on the figures show RA (x-axis) and DEC (y-axis). The brightness of the three images are separately scaled.

in each channel range were calculated using the same extraction radius as the combined spectrum. The nebular spectrum was created by replacing the counts in the re-binned combined spectrum (see Figure 2). The same background spectrum is used for both the combined and the nebular spectral analysis.

The nebular X-ray spectrum was modeled using a two-component plasma emission model with two different hydrogen column densities (i.e.,  $tbabs*MEKAL+tbabs*MEKAL$  or  $tbabs*PSHOCK+tbabs*PSHOCK$ ) since a single plasma model or a single absorption component yielded  $\chi^2_\nu$  larger than 2 ( $tbabs$ –Wilms et al. 2000; MEKAL– Mewe et al. 1986; PSHOCK–Borkowski et al. 2001). The fits with the power-law and two-temperature non-equilibrium ionization plasma models (e.g., NPSHOCK–Borkowski et al. 2001) resulted in either a large  $\chi^2_\nu$  with the single component model fits or similar  $\chi^2_\nu$  with the two-component model fits, yielding non-physical spectral parameters (e.g., too high temperatures or negative photon indices). Note that T Pyx is not a radio source in quiescence. Table 1 shows the spectral parameters for two-component plasma model fits with a MEKAL model (assuming collisional equilibrium) and a PSHOCK model (assuming non-equilibrium ionization). The fits yield similar parameters. The ionization timescales derived from the PSHOCK model indicate existence of non-equilibrium ionization plasma, but the parameter can not be constrained allowing for ionization equilibrium. The spectral results (e.g., Double MEKAL) indicate an absorbed X-ray flux of  $(0.6-10.0)\times 10^{-14}$  erg s $^{-1}$  cm $^{-2}$  which translates to an X-ray luminosity of  $(0.08-2)\times 10^{32}$  erg s $^{-1}$  at the source distance of 3.5 kpc (distance from Selvelli et al. 2008).

In order to determine the central source spectrum, I fitted the combined spectrum with a composite model ( $tbabs*MEKAL+tbabs*MEKAL+tbabs*MEKAL$ ). The two MEKAL models (with the two different absorption models) represent the nebular spectrum and the last is used to model the central binary spectrum typical of accreting CVs. I fixed the nebular spectrum parameters at their best fit values (second  $N_H$  slightly varied) and fitted the composite model to the combined spectrum. The fitted combined spectrum is displayed in the bottom panel of Figure 2. As a result, I derive an  $N_H$  of  $0.03^{+0.15}_{\geq} \times 10^{22}$  cm $^{-2}$ , a kT of  $9.2^{_{-5.4}_{\leq}}$  keV, and a normalization of  $1.5^{+1.0}_{-0.8} \times 10^{-5}$  for the spectrum of the central source emission. This yields an X-ray flux of  $(1.0-5.8)\times 10^{-14}$  erg s $^{-1}$  cm $^{-2}$  with a luminosity of  $(1.4-8.2)\times 10^{31}$  erg s $^{-1}$ . The count rate error of 40% in the subtraction of the nebular component is quadratically added to the normalization, flux and luminosity. Note that the  $N_H$  value of the central source and the first component of the X-ray emitting nebula are in good agreement with the measured value of  $E(B-V)=0.5$  (Shore et al. 2011) which yields an interstellar  $N_H$  of  $3\times 10^{21}$  cm $^{-2}$ .

Table 1: Spectral Parameters of the Nebular Spectrum of T Pyx (0.2-9.0 keV); ranges correspond to  $2\sigma$  errors ( $\Delta\chi^2= 3.84$  – single parameter) for the first and  $3\sigma$  errors ( $\Delta\chi^2= 6.63$  – single parameter) for the second component;  $\chi^2_\nu$  values of the fits are  $\leq 1.0$ .

	PSHOCK § <sup>1</sup>	MEKAL § <sup>2</sup>
$N_{\text{H1}} (\times 10^{22} \text{ cm}^{-2})$	$0.4^{+0.25}_{-0.2}$	$0.5^{+0.4}_{-0.3}$
$kT_{s1}^a (\text{keV})$	$1.0^{+1.1}_{-0.4}$	$0.6^{+0.3}_{-0.3}$
$\tau_1^b (\times 10^{11} \text{ s cm}^{-3})$	$\sim 3.2$	N/A
$K_1^{c,d} (\times 10^{-5} \text{ cm}^{-5})$	$0.6^{+0.3}_{-0.5}$	$0.6^{+0.3}_{-0.3}$
$N_{\text{H2}} (\times 10^{22} \text{ cm}^{-2})$	$11.5^{+22.5}_{-7.3}$	$17.0^{+9.7}_{-14.0}$
$kT_{s2}^a (\text{keV})$	$2.3 <$	$2.2^{+2.0}_{-1.2}$
$\tau_2^b (\times 10^{11} \text{ s cm}^{-3})$	$\sim 2$	N/A
$K_2^{c,d} (\times 10^{-5} \text{ cm}^{-5})$	$3.5^{+5.2}_{-1.7}$	$9.8^{+23.0}_{-7.5}$

§<sup>1</sup>The fitted model is (*tbabs*\*PSHOCK+*tbabs*\*PSHOCK) using two different  $N_{\text{H}}$  parameters.

§<sup>2</sup>The fitted model is (*tbabs*\*MEKAL+*tbabs*\*MEKAL) using two different  $N_{\text{H}}$  parameters.

<sup>a</sup>1 keV  $\simeq 1.2 \times 10^7 K$ .

<sup>b</sup> $\tau = n_0 t$

<sup>c</sup>The normalization constant of the MEKAL/PSHOCK plasma emission models  $K=(10^{-14}/4\pi D^2)\times \text{EM}$  where EM (Emission Measure) =  $\int n_e n_H dV$  (integration is over the emitting volume V).

<sup>d</sup>a propagated count rate error of 40% is quadratically added.

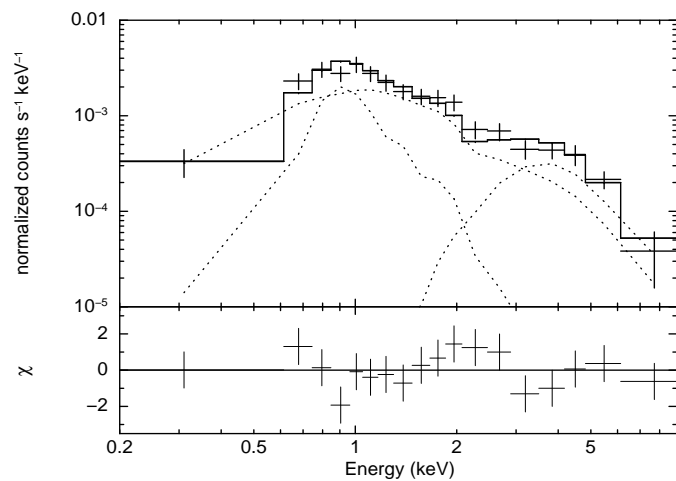
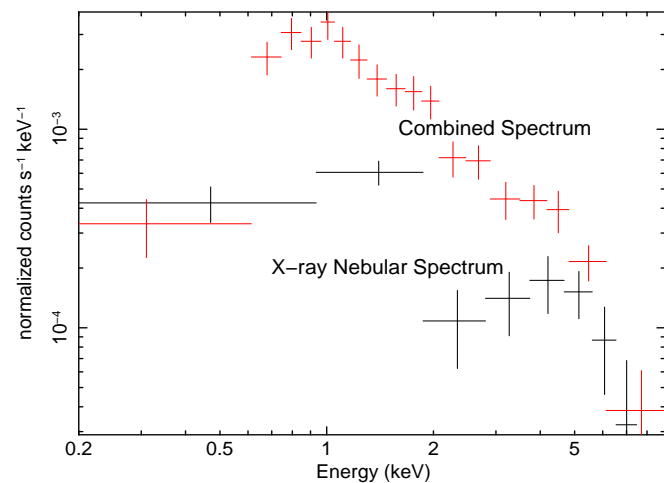


Fig. 2.— The top panel shows the combined/total spectrum of the source plus the nebular emission in the X-rays (in red) and the nebular X-ray spectrum around T Pyx (in black). The bottom panel shows the Chandra ACIS-S combined spectrum fitted with ( $tbabs*MEKAL+tbabs*MEKAL+tbabs*MEKAL$ ) model of emission. The dotted lines show the contribution of the three fitted MEKAL models. The lower panel shows the residuals between the data and the total model in standard deviations.

### 3.3. The Temporal Variations of the Central Source

I created background-subtracted light curves with the aid of the CIAO task *dmextract* to search for any time variability. The three light curves were, then, used to generate averaged power spectra (PSD). I find significant modulations at  $0.155 \pm 0.005$  mHz which is the binary period of the system (and its second harmonic) above 99.9% confidence level (see Figure 3) where the  $3\sigma$  power threshold is  $> 77$  taking into account the red noise in the PSD. The binary period is 1.8295(3) hrs; 0.152 mHz (Uthas et al. 2010). Note that there is a constant level of emission in the folded light curve at about  $0.003 \text{ c s}^{-1}$  (see Figure 3 right hand panel). Superimposed on this constant level, there is a variation between 0.003 and  $0.008 \text{ c s}^{-1}$  with a mean, *net*, count rate of  $0.0025 \text{ c s}^{-1}$ . These rates are in accordance with the rates I derive for the X-ray nebula and the central source, respectively.

## 4. Discussion

The imaging results indicate the existence of a torus-like or ring-like elliptical structure around T Pyx which most likely suffers projection effects. If one assumes a simple circular region viewed along a given line of sight (inclination) angle ( $R \sin(i) =$  semi-minor axis) taking  $R=0''.9$  and semi-minor axis as  $0''.4$ , one finds an inclination angle of  $i \leq 27^\circ$ . The inclination of the binary system is about  $10^\circ$  (Uthas et al. 2010). On the other hand, the elliptical structure could be a complicated projection effect of a conical face-on bipolar ejection interacting with a large spherical shell, where the cut plane will be in the form of an ellipse. The images of the nebula in the total and 1-2 keV band (see Figure 1) hint at such effects plus an elongation towards the south of  $1''.8-1''.9$ . It is possible that this is a part of a bipolar ejection and/or a jet-like outflow from the nova.

The structure in the X-ray nebula is consistent with the detection of a face-on bipolar ejection detected in the 2011 outburst of T Pyx using the near-infrared observations (Chesneau et al. 2011). The orientation of the [NII]+H $\alpha$  (HST) images, mostly composed of knots, also show a north to south elongation from the source position (Shara et al. 1997) consistent with the *Chandranebula* at a larger extend. The small size of the X-ray nebula indicates that it most likely results from an interaction of the 1966 ejecta with the pre-existing shells/older ejecta. The size of the torus-like structure  $\sim 0''.9$  (a possible minimum due to projection effects) yields an expansion velocity of  $V_{exp} \geq 400 D_{3.5kpc} \text{ km s}^{-1}$ .

The extended emission in T Pyx was detected using an archival *XMM-Newton* EPIC pn observation obtained in 2006 (Balman 2010). However, the low pixel resolution ( $4''$ ) and the large PSF size (half energy radius  $\sim 6''-7''$ ; Strüder et al. 2001), hindered the spatial

deconvolution and only distortion in the radial profiles were recovered. The extension in the EPIC pn image in slight excess of 15'' is consistent with the HRMA+EPIC pn PSF half energy width of 15''. Similarly, Chandra ACIS-S PSF has a half energy radius  $\sim 0''.418$  and the *Chandra* nebula (+southern elongation) is in slight excess of the HEW making the two detections consistent. The south/southwest elongation in both detections are also in accordance given the differences in the instrument characteristics.

The spectral deconvolution shows two different plasma emission components from the nova remnant. The calculated emission measure  $EM = \langle n_e \rangle^2 V_{eff}$ , obtained from the normalization of the fit, yields an average electron density  $n_e$  of about  $32 \text{ cm}^{-3}$  and  $115 \text{ cm}^{-3}$  for the colder and hotter plasma, respectively. A volume of  $6.7 \times 10^{50} \text{ cm}^3$  is used (consistent with a spherical region of 1'' radius at 3.5 kpc) and a filling factor  $f=1$  ( $V_{eff}=f \times V$ ) is assumed. If the filling factor is as small as  $1 \times 10^{-2}$ , then the electron density can be as high as  $320 \text{ cm}^{-3}$  and  $1150 \text{ cm}^{-3}$ . The non-equilibrium ionization model (PSHOCK) indicate  $n_e \sim 100 \text{ cm}^{-3}$ . The electron density in the X-ray nebula of GK Per was found in a range  $0.6\text{-}11.0 \text{ cm}^{-3}$  for  $f=1$  (Balman 2005) and smaller than for T Pyx.

The shocked mass in the X-ray nebula of T Pyx can be approximated as  $< 1.8 \times 10^{-5} M_\odot$  assuming a fully ionized gas, and  $M_{neb} \simeq n_e m_H V_{eff}$ . By comparison, Selvelli et al. (2008) have calculated an ejecta mass of  $10^{-4}\text{-}10^{-5} M_\odot$  for the 1966 outburst. Shore et al. (2011) measured an ejecta mass of  $< 1 \times 10^{-5} M_\odot$  ( $f=1$ ) for the 2011 outburst. The plasma temperature derived from the fits can be used to approximate the shock velocities using the strong shock relation  $kT_s = (3/16) \mu m_H (v_s)^2$ , ( $T = 1.4 \times 10^5 v_{100 \text{ km s}^{-1}}^2$ ). I derive about 500-870  $\text{km s}^{-1}$  for the first component consistent with the minimum speed calculated from the size of the X-ray nebula and the expansion speeds of the 1966 outburst that are in the range 850-2000  $\text{km s}^{-1}$  (Catchpole 1969). I suggest that the first plasma component is the forward shock and the second embedded component is possibly due to the reverse shock.

Contini & Prialnik (1997) have modeled the circumstellar interaction of the T Pyx shells finding that as the latest shell catches the older shell already decelerated by the circumbinary medium a forward shock moves into the older ejecta and a reverse shock moves into the new ejecta. Typical densities they derive are about  $\sim 200 \text{ cm}^{-3}$  and  $\sim 3000 \text{ cm}^{-3}$  for the forward and reverse shock zones. The model predicts a faster and hotter reverse shock than the forward shock. *Chandra* results are in reasonable agreement with these predictions. However, the ejecta have not swept up significantly more than their own mass, which makes the shell a Sedov remnant. There is a neutral hydrogen column density difference of about 10 times between the two plasma components of T Pyx which was similar to the X-ray nebula of GK per. This could be an absorption in a thin cold shell (e.g., between the forward and reverse shocks) or ionized absorption with possibly non-solar abundances (see also Balman 2005).

An ionized warm absorption column density, equivalent to cold absorption (by hydrogen) column density of  $1 \times 10^{23} \text{ cm}^{-2}$ , can be a factor of 10 less  $\sim$  a few  $\times 10^{22} \text{ cm}^{-2}$  (see Pekön & Balman 2012). This two-component plasma model may, possibly, be an effect of an X-ray emitting non-equilibrium plasma in the nova ejecta that needs modeling.

Selvelli et al. (2008) predict an accretion luminosity of  $10^{35} \text{ erg s}^{-1}$  in the X-rays for T Pyx consistent with the calculated accretion rates. The accretion luminosity is about 100-500 times more than the X-ray luminosity I detect for the central source revealing a different origin of X-ray emission than accretion (i.e., boundary layer) (similar to the *XMM-Newton* results). I suggest that the X-rays from the point source originate from an accretion disk corona (i.e., or an ADAF zone) in the system. Although, the X-ray luminosity is consistent with the X-ray emission from stellar winds, the temperature is too high for such an interpretation. The orbital modulation can be caused by scattering of the X-rays from structures fixed in the orbital plane.

The author thank the *Chandra* Observatory for performing the observations of T Pyx. SB thanks S. Starrfield, J.J. Drake, M. Bode, J. Krautter, M. Hernanz, J-U. Ness for critical reading of the manuscript and valuable discussions. SB acknowledges support from TÜBİTAK, The Scientific and Technological Research Council of Turkey, through project 108T735.

## REFERENCES

- Balman, Ş. 2010, MNRAS, 404, L26
- Balman, Ş. 2005, ApJ, 627, 933
- Balman, Ş., & Ögelman, H. B. 1999, ApJ, 518, L111
- Balman, Ş., Krautter, J., & Ögelman, H. 1998, ApJ, 499, 395
- Bode, M. F., & Evans, A. 2008, Classical Novae (Classical Novae, 2nd Edition. Edited by M.F. Bode and A. Evans. Cambridge Astrophysics Series, No. 43, (Cambridge: Cambridge University Press)
- Bode, M. F. et al. 2006, ApJ, 652, 629
- Borkowski, K.J., Lyerly, W.J., Reynolds, S.P. 2001, ApJ, 548, 820
- Catchpole, R. M. 1969, MNRAS, 142, 119
- Chesneau, O. et al. 2011, A&A, 534, L11
- Contini, M., & Prialnik, D. 1997, ApJ, 475, 803

- Drake, J. J. et al. 2009, *ApJ*, 691, 418
- Garmire, G., Feigelson, E.D., Broos, P., Hillenbrand, L.A., Townsley, L., & Tsuboi, Y. 2000, *AJ*, 120, 1426
- Gilmozzi, R., & Selvelli, P. 2007, *A&A*, 461, 593
- Hernanz, M., & Sala, G. 2002, *Science*, 298, 393
- . 2007, *ApJ*, 664, 467
- Krautter, J., 2008, in *Classical Novae*, eds Bode M.F. & Evans A., Wiley, Cambridge University Press, Second edition, Chapt. 10
- Kuulkers, E. et al. 2011a, *Astronomer’s Telegram* 3285
- Kuulkers, E. et al. 2011b, *Astronomer’s Telegram* 3647
- Livio, M. 1994, in *Interacting Binaries*, Saas-Fee Advanced Course 22, ed. H. Nussbaumer & A. Orr (Berlin: Springer), 135
- Luna, G.J., Montez, R., Sokoloski, J.L., Mukai, K., & Kastner, J.H. 2009, *ApJ*, 707, L1168
- Mewe, R., Lemen, J. R., & van den Oord, G. H. J. 1986, *A&AS*, 65, 511
- Mukai, K., & Ishida, M. 2001, *ApJ*, 551, 1024
- Nelson, T., Donato, D., Mukai, K., Sokoloski, J., & Chomiuk, L. 2012, *ApJ*, 748, 43
- Ness, J.-U. et al. 2009, *AJ*, 137, 3414
- O’Brien, T. J., & Cohen, J. G. 1998, *ApJ*, 498, L59
- Orio, M. et al. 2001, *MNRAS*, 326, L13
- Orlando, S., & Drake, J. J. 2012, *MNRAS*, 419, 2329
- Page, K. L. et al. 2010, *MNRAS*, 401, 121
- Pekön, Y. & Balman, S. 2012, *AJ*, 144, 53
- Schaefer, B. E., Pagnotta, A., Shara, M. M. 2010, *ApJ*, 708, 381
- Selvelli, P., Cassatella, A., Gilmozzi, R., & González-Riestra, R. 2008, *A&A*, 492, 787
- Shara, M. M. 1989, *PASP*, 101, 5
- Shara, M. M., Moffat, A., Williams, R.E., & Cohen, J. 1989, *ApJ*, 337, 720
- Shara, M. M., Zurek, D. R., Williams, R. E., Prialnik, D., Gilmozzi, & R., Moffat A. F. J. 1997, *AJ*, 114, 258
- Shore, S.N., Augusteijn, T., Ederoclite, A., & Uthas, H. 2011, *A&A*, 533, L8
- Sokoloski, J. L., Luna, G. J. M., Mukai, K., & Kenyon, S. J. 2006, *Nature*, 442, 276

- Starrfield, S. 2001, in ASP Conf. Ser. 231, Tetons 4: Galactic Structure, Stars, and the Interstellar Medium, C.E. Woodward, M.D. Bica, & J.M. Shull (eds), (San Francisco: ASP), p. 466
- Strüder, L. et al. 2001, A&A, 365, L18
- Uthas, H., Knigge, C., & Steeghs, D. 2010, MNRAS, 409, 237
- Vaytet, N. M. H., O’Brien, T. J., Page, K. L., Bode, M. F., Lloyd, M., & Beardmore, A.P. 2011, ApJ, 740, 5
- Waagan, E. et al. 2011, CBET, 2700, 1
- Webbink, R. F., Livio, M., Truran, J. W., & Orio, M. 1987, Ap&SS, 131, 493
- Weisskopf, M., O’dell, Stephen, L., van Speybroeck, L.P., 1996, SPIE, 2805, 2
- Wilms, J., Allen, A., & McCray, R. 2000, ApJ, 542, 914

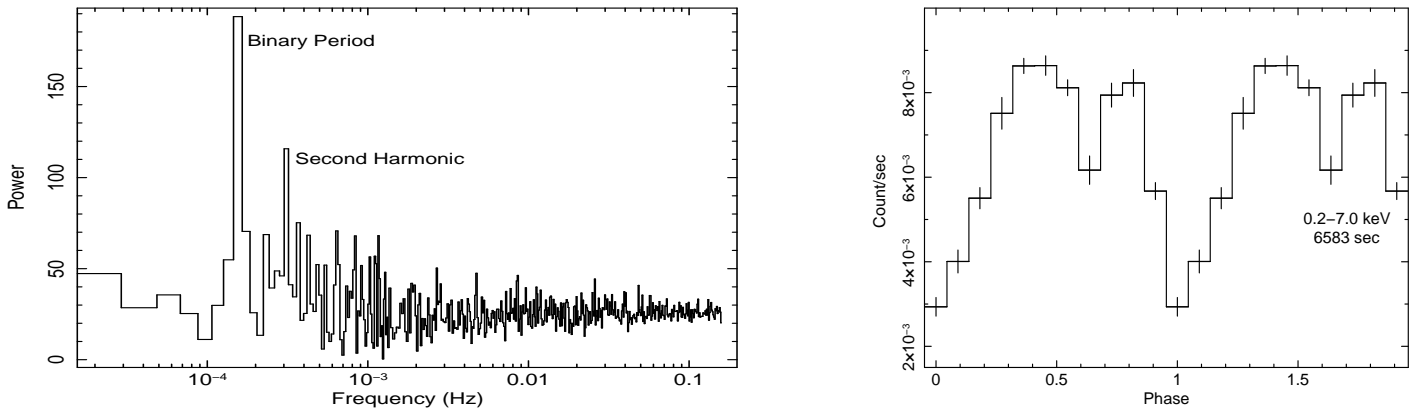


Fig. 3.— The left hand panel shows the PSD obtained from averaged power spectra of the three observations of T Pyx. The binary period and its second harmonic are labeled. The right hand panel is the folded average X-ray light curve of T Pyx using the detected binary period.